

Multifunctional Conjugates To Prepare Nucleolar-Targeting CdS Quantum Dots

Ran Shen,[†] Xiaoqin Shen,[†] Zengming Zhang,[‡] Yuesheng Li,[§] Shiyong Liu,[†] and Hewen Liu^{*†}

CAS Key Laboratory of Soft Matter Chemistry, Department of Polymer Science and Engineering, and Department of Astronomy and Applied Physics, University of Science and Technology of China, Hefei, Anhui 230026, China, and State Key Laboratory of Polymer Physics and Chemistry, Changchun Institute of Applied Chemistry, Changchun 130022, China

Received January 12, 2010; E-mail: lhewen@ustc.edu.cn

Abstract: We used a click reaction to synthesize a bidentate 1,2,3-triazole-based ligand, TA, for use in the preparation of aqueous CdS quantum dots (QDs). TA-conjugated CdS QDs exhibited two fluorescence emission peaks, one at 540 nm arising from CdS nanocrystals and the other at ~670 nm arising from TA–CdS QD complexes formed via surface coordination. Coordination between TA and CdS was verified by using X-ray photoelectron (N 1s) spectra as well as Raman and NMR spectra of TA-capped QDs. Electrochemical analysis revealed that the 1,2,3-triazole moieties in TA form complexes with the Cd(II) ions. The aqueous QDs protected by TA were very stable at different ionic strengths and over a broad pH range, according to fluorescence analysis. The ethidium bromide exclusion assay demonstrated that the bidentate TA ligand interacts strongly with DNA. Fluorescent micrographs and TEM images of cancer cells stained with TA-capped QDs clearly showed that the TA ligand targeted CdS QDs to the nucleoli of cells. In contrast, thioglycolic acid-capped CdS QDs just stained the cell membranes and could not pass the cell membranes to reach the cell nucleus.

Introduction

Semiconductive quantum dots (QDs) have emerged as promising fluorescent probes in biological and medical fields such as bioassays, cell imaging, and clinic diagnosis.^{1–3} One of the keys to the successful use of QDs in biosystems is the ability to tailor their surface properties with ligands to achieve hydrophilicity and aqueous stability and to target QDs to specific biomolecules or organelles, such as cell nuclei, especially nucleoli. The nucleolus is increasingly recognized as a critical regulator of many cellular functions and is also emerging as an important target of various viral proteins (e.g., the HIV virus).⁴ Nuclear and nucleolar targeting of nanoparticles in cells is generating widespread interest. However, discovery of nucleolar targeting signals (NoLSs) remains a challenge. Most of the

identified NoLSs are complicated polypeptides or proteins isolated from viruses.⁵ The motifs that are involved in regulating nucleolar localization do not seem to be well-defined and remain largely unknown.⁴

Because of the growing importance of QDs in biology, numerous ligands and strategies for preparing QD bioconjugates have been developed.^{1–3,6} The most widely used ligands are based on the substitution of native tri-*n*-octylphosphine/tri-*n*-octylphosphine oxide (TOP/TOPO) or thiol-containing chemicals, including dihydrolipoic acid (DHLA), which can interact with the surface of QDs as strongly as covalent bonds.⁷ Some other ligands, such as cationic multivalent polyamine, have also been used recently through ligand-exchange methods.^{8,9} However, these approaches commonly require multiple steps or oxygen-sensitive chemicals to obtain the final products.

[†] CAS Key Laboratory of Soft Matter Chemistry, University of Science and Technology of China.

[‡] Department of Astronomy and Applied Physics, University of Science and Technology of China.

[§] State Key Laboratory of Polymer Physics and Chemistry, Changchun Institute of Applied Chemistry.

(1) Medintz, I. L.; Uyeda, H. T.; Goldman, E. R.; Mattoussi, H. *Nat. Mater.* **2005**, *4*, 435–446.

(2) Chan, W. C. W.; Nie, S. *Science* **1998**, *281*, 2016–2018.

(3) Michalet, X.; Pinaud, F. F.; Bentolila, L. A.; Tsay, J. M.; Doose, S.; Li, J. J.; Sundaresan, G.; Wu, A. M.; Gambhir, S. S.; Weiss, S. *Science* **2005**, *307*, 538–544.

(4) (a) Nosaka, T.; Siomi, H.; Adachi, Y.; Ishibashi, M.; Kubota, S.; Maki, M.; Hatanaka, M. *Proc. Natl. Acad. Sci. U.S.A.* **1989**, *86*, 9798–9802. (b) Volmer, R.; Mazel-Sanchez, B.; Volmer, C.; Soubies, S. M.; Guérin, J.-L. *Virol. J.* **2010**, *7*, 63–67. (c) Hatanaka, M. *BioEssays* **2005**, *12*, 143–148. Emmott, E.; Hiscox, J. A. *EMBO Rep.* **2009**, *10*, 231–238. (d) Lixin, R.; Efthymiadis, A.; Henderson, B.; Jans, D. A. *Biochem. Biophys. Res. Commun.* **2001**, *284*, 185–193.

(5) (a) Kalland, K.-H.; Szilvay, A. M.; Brokstad, K. A.; Saetrevik, W.; Haukenes, G. *Mol. Cell. Biol.* **1994**, *14*, 7436–7444. (b) Dang, C. V.; Lee, W. M. F. *J. Biol. Chem.* **1989**, *264*, 18019–18023.

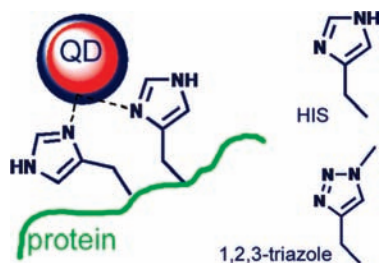
(6) Michalet, X.; Pinaud, F. F.; Bentolila, L. A.; Tsay, J. M.; Doose, S.; Li, J. J.; Sundaresan, G.; Wu, A. M.; Gambhir, S. S.; Weiss, S. *Science* **2005**, *307*, 538–544.

(7) In addition to those mentioned in refs 1–3 and 6, see the following recent references: TOP/TOPO ligands: (a) Sudeep, P. K.; Early, K. T.; McCarthy, K. D.; Odoi, M. Y.; Barnes, M. D.; Emrick, T. *J. Am. Chem. Soc.* **2008**, *130*, 2384–2385. (b) Dubertret, B.; Skourides, P.; Norris, D. J.; Noireaux, V.; Brivanlou, A. H.; Libchaber, A. *Science* **2002**, *298*, 1759–1762. DHLA ligands: (c) Uyeda, H. T.; Medintz, I. L.; Jaiswal, J. K.; Simon, S. M.; Mattoussi, H. *J. Am. Chem. Soc.* **2005**, *127*, 3870–3878. (d) Susumu, K.; Uyeda, H. T.; Medintz, I. L.; Pons, T.; Delehanty, J. B.; Mattoussi, H. *J. Am. Chem. Soc.* **2007**, *129*, 13987–13996.

(8) Duan, H.; Nie, S. *J. Am. Chem. Soc.* **2007**, *129*, 3333–3338.

(9) Dubois, F.; Mahler, B.; Dubertret, B.; Doris, E.; Mioskowski, C. *J. Am. Chem. Soc.* **2007**, *129*, 482–483.

Scheme 1. Metal-Affinity Coordination of HIS to a QD Surface

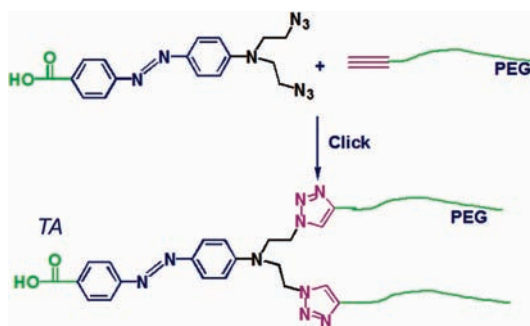


A new group of interesting multifunctional biological ligands are histidine (HIS)-expressing proteins or peptides, which can be used to cap QDs through metal-affinity coordination of HIS residues to metal atoms on the QD surface for simultaneous aqueous dispersion and biofunctionalization (Scheme 1); this is a well-known, versatile method developed by Mattoussi's group.¹⁰ Surface coordination may generate new fluorescent complexes that can supply possibilities for modulation of the fluorescence properties of QDs. Furthermore, the surface coordination approach has the flexibility for the design of the molecular structures of charge donors/acceptors. Though the ligands via surface coordination may have interactions with the QD surface that are weaker than covalent bonds, multidentate ligands can overcome this shortcoming.

Very recently, "click" chemistry became an important chemical approach for the design of drug molecules and macromolecules.¹¹ Click chemistry is also a convenient way to afford the 1,2,3-triazole group. In the course of studying click chemistry for the construction of macromolecules with controlled structures,¹² we realized that the 1,2,3-triazole group can serve as a HIS-like conjugate for stabilization and functionalization of fluorescent QDs. 1,2,3-Triazole ligands synthesized through click reactions have been found to form complexes with some late transition-metal ions.¹³ However, application of click ligands for aqueous QDs has not been reported to date. In comparison with HIS ligands, the concept of click chemistry is more "synthetic" and thus more controllable.

Herein, we present the design and preparation of new, stable colloidal CdS QDs utilizing a bidentate 1,2,3-triazole-based ligand, TA, appended with poly(ethylene glycol) (PEG). The surface coordination of TA to CdS generates a new red

Scheme 2. Synthesis of the Bidentate Ligand TA



fluorescence peak in addition to the olivine photofluorescence peak of CdS nanocrystals. Thus, TA-capped CdS QDs are a new kind of dual-colored QDs dependent on excitation, which must be an interesting feature for simultaneous multicolor imaging. For the purpose of multiplexing, we introduced an azobenzene group in the ligands to investigate the photoswitchability of the photofluorescence. We also demonstrated that the bidentate TA ligand strongly interacts with DNA, as evidenced by a new photofluorescence peak upon complexation with DNA and by the ethidium bromide exclusion assay. The TA-capped CdS QDs show an unexpected strong affinity to cell nucleoli. The structure of the TA ligand may provide clues on the design of new antivirus drugs. Thus, the new TA ligand allows the design of CdS nanocrystals that are water-soluble and multifunctional.

Results and Discussion

Design and Synthesis of the TA Ligand. In this work, we designed the bidentate ligand azobenzobis(1,2,3-triazole-PEG) (TA), as elucidated in Scheme 2. The two 1,2,3-triazole groups were incorporated to strongly interact with the surface of QDs. The carboxylic groups are conducive to binding of TA to QDs as well. The polyethylene glycol (PEG) tails confer water solubility and biocompatibility. We introduced the azobenzene moiety in the TA ligand to achieve photoswitchable fluorescence properties that could be useful for signal multiplexing and to serve as a hydrophobic end that could enhance adsorption of TA to QDs in aqueous media. TA was quite soluble in water. The synthesis and structural characterization are presented in the Supporting Information.

CdS QDs were produced in aqueous solutions of TA with TA/Cd(II) molar ratios of 6, 8, 10, and 12. At a TA/Cd(II) molar ratio of 10, the fluorescence intensity due to complexation of TA with Cd atoms on the CdS QD surface was the highest (see Figure 2B). Thus, we utilized CdS QDs that were produced in aqueous solutions with TA/Cd(II) = 10 in subsequent studies, unless another TA/Cd(II) ratio is specifically mentioned. X-ray diffraction (XRD) analysis showed that the crystalline structures of the obtained CdS QDs were hexagonal (Figure S1 in the Supporting Information). The diameters of the QDs were calculated to be 2.0 nm on the basis of the full width at half-maximum (FWHM) values of the (110) and (112) XRD planes according to Scherrer equation.¹⁴

The microstructure of TA-capped CdS was investigated using transmission electron microscopy (TEM) (Figure 1A). The particle size observed by means of TEM was ~2 nm, which is

- (10) For studies involving HIS ligands, see: (a) Medintz, I. L.; Clapp, A. R.; Mattoussi, H.; Goldman, E. R.; Fisher, B.; Mauro, J. M. *Nat. Mater.* **2003**, *2*, 630–638. (b) Medintz, I. L.; Clapp, A. R.; Brunel, F. M.; Tiefenbrunn, T.; Uyeda, H. T.; Chang, E. L.; Deschamps, J. R.; Dawson, P. E.; Mattoussi, H. *Nat. Mater.* **2006**, *5*, 581–589. (c) Delehanty, J. B.; Medintz, I. L.; Pons, T.; Brunel, F. M.; Dawson, P. E.; Mattoussi, H. *Bioconjugate Chem.* **2006**, *17*, 920–927. (d) Slocik, J. M.; Moore, J. T.; Wright, D. W. *Nano Lett.* **2002**, *2*, 169–173. (e) Hainfeld, J. F.; Liu, W.; Halsey, C. M. R.; Freimuth, P.; Powell, R. D. *J. Struct. Biol.* **1999**, *127*, 185–198.
- (11) Rostovtsev, V. V.; Green, L. G.; Fokin, V. V.; Sharpless, K. B. *Angew. Chem., Int. Ed.* **2002**, *41*, 2596–2599.
- (12) (a) Ge, Z.; Zhou, Y.; Xu, J.; Liu, H.; Chen, D.; Liu, S. *J. Am. Chem. Soc.* **2009**, *131*, 1628–1629. (b) Peng, Y.; Liu, H.; Zhang, X.; Liu, S.; Li, Y. *Macromolecules* **2009**, *42*, 6457–6462. (c) Shen, X.; Liu, H.; Li, Y.; Liu, S. *Macromolecules* **2008**, *41*, 2421–2425.
- (13) (a) Fletcher, J. T.; Bumgarner, B. J.; Engels, N. D.; Skoglund, D. A. *Organometallics* **2008**, *27*, 5430–5433. (b) Suijkerbuijk, B. M. J. M.; Aerts, B. N. H.; Dijkstra, H. P.; Lutz, M.; Spek, A. L.; van Koten, G.; Gebbink, R. J. M. K. *Dalton Trans.* **2007**, 1273–1276. (c) Mukai, H.; Sohrin, Y. *Inorg. Chim. Acta* **2009**, *362*, 4526–4533. (d) Beyer, B.; Ulbricht, C.; Escudero, D.; Friebe, C.; Winter, A.; Gonzalez, L.; Schubert, U. S. *Organometallics* **2009**, *28*, 5478–5488. (e) Monkowius, U.; Ritter, S.; König, B.; Zabel, M.; Yersin, H. *Eur. J. Inorg. Chem.* **2007**, 4597–4606.

- (14) Compagnini, G.; Fragala, M. E.; D'Urso, L.; Spinella, C.; Puglisi, O. *J. Mater. Res.* **2001**, *16*, 2934–2938.

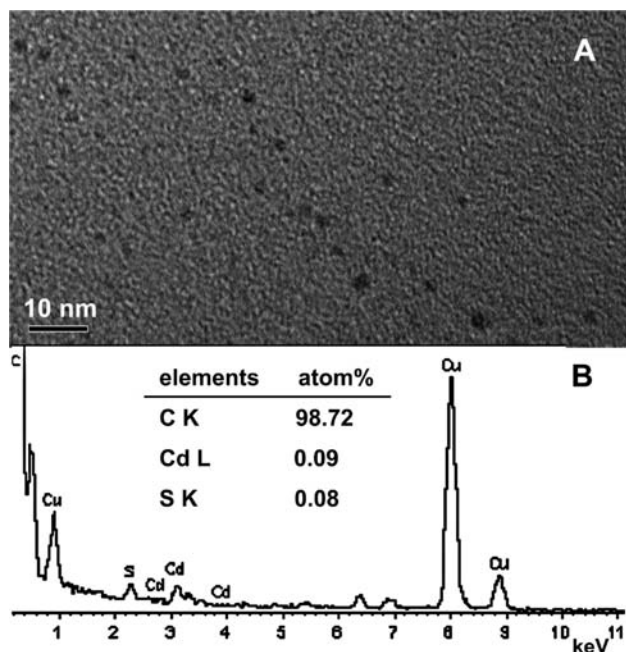


Figure 1. (A) TEM image and (B) EDS analysis of TA-capped QDs on a carbon-coated copper mesh grid.

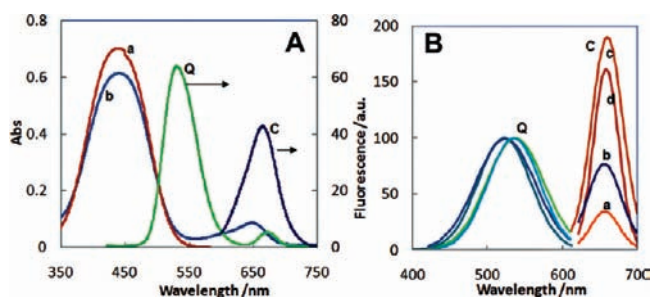


Figure 2. UV-vis absorption and fluorescence spectra. (A) UV-vis spectra of (a) TA and (b) TA-capped CdS QDs and fluorescence spectra of TA-capped CdS QDs excited at (Q) 390 and (C) 590 nm. (B) Fluorescence spectra of TA-capped CdS QDs produced with TA/Cd(II) molar ratios of (a) 6, (b) 8, (c) 10, and (d) 12. The peaks of band Q in (B) have been normalized, and the intensities of band C are relative to band Q.

consonant with the results from XRD. Energy dispersive X-ray (EDS) analysis showed that the Cd/S atom ratio was 1:1 (Figure 1B).

Absorption and Fluorescence Properties of TA-Capped CdS QDs. The TA ligand in water showed a single absorption peak in the range from 350 to 750 nm (a in Figure 2A). This peak, at ~ 450 nm, arises from azobenzene and overlapped the absorption peak of CdS nanocrystals with size smaller than 4 nm, as determined according to the Brus equation.¹⁵ TA-capped CdS QDs had two absorption peaks, one at 450 nm and a newly appearing one at ~ 650 nm that arose from the formation of the complexes of TA and surface Cd atoms (b in Figure 2A). More experimental results are presented in this work to prove the formation of the complexes of TA and surface Cd atoms.

Photofluorescence analysis was performed. The TA ligand did not show any significant fluorescence in the UV-vis range at all, whereas TA-capped CdS QDs exhibited two fluorescence emission peaks at ~ 540 and 670 nm (bands Q and C,

Table 1. Quantum Yields of TA-Capped CdS QDs

quantum yield (%)		medium	azobenzene isomerization conditions
band Q	band C		
17.5	74.5	H ₂ O	visible light
20.5	95.8	THF	visible light
10.6	95.8	THF	in darkness
17.0	95.8	THF	UV

respectively, in Figure 2). Band Q was emitted from CdS nanocrystals with a continuous excitation spectrum, whereas band C had a maximum excitation peak at ~ 650 nm. The intensity of band C relative to band Q increased with increasing TA/Cd molar ratio and reached a maximum at TA/Cd = 10, which indicated that band C is related to the surface complexes of TA. As TA/Cd increased, band Q was blue-shifted, meaning that higher ligand concentrations favored smaller particles.

We measured the quantum yields of the two fluorescence bands and found 17.5 and 74.5% for bands Q and C, respectively, in aqueous solutions. The quantum yields of band C increased to 95.8% in an organic solvent such as tetrahydrofuran (THF) (Table 1). The quantum yields of most aqueous QDs reported in the literature are 3–30%.

TA-capped CdS QDs are a new kind of dual-colored QDs dependent on excitation, emitting an olive color under UV or blue-light excitation, due to the broad and continuous excitation spectrum of nanocrystalline CdS, while emitting red light (~ 670 nm) under excitation using green light. Differing from general QDs, TA-capped CdS QDs changed colors in situ when the excitation was changed. Multicolor imaging of different bio-materials in a cell has become a fundamental technique in cell biology during the past decade. Longer-wavelength dyes could become valuable tools, as these dyes expand the range of options for multicolor detection. Furthermore, the red and far-red dyes could be excited with longer, less cytotoxic wavelengths and emitted at wavelengths longer than the usual sources of cell autofluorescence, resulting in a higher signal-to-noise ratio.

Photoswitchability of certain fluorescence would be useful for multicolor imaging. Thus, we introduced the azobenzene group in TA. Azobenzene undergoes mutual isomerization between the cis and trans isomers. Under UV irradiation, azobenzene adopts the cis conformation, whereas its conformation reverts back to the trans form upon exposure to visible light.

However, the TA-capped CdS QDs did not show significant photoresponsivity in aqueous solutions, possibly as a result of adsorption of azobenzene groups on the QD surface or H-aggregation among the azo groups.¹⁶ In contrast, in an organic solvent (e.g., acetone, THF, or DMSO), the TA ligand and the TA-capped CdS QDs were responsive to different illumination. Acetone and DMSO are common organic solvents for biological experiments. It was found that band Q of the CdS QDs showed reversible photoswitchability against the photoisomerization of azobenzene groups in organic solutions (Figure 3); in contrast, however, fluorescence band C kept a constant intensity (Table 1). The overlap of the absorption peak of TA in the cis form and that of CdS was attributed to the photoresponsivity of fluorescence band Q. When TA was in the cis form, it would shade the QDs from light energy that CdS could absorb. The photoresponsivity results also indicated that fluorescence band

(15) Pesika, N. S.; Stebe, K. J.; Searson, P. C. *J. Phys. Chem. B* **2003**, *107*, 10412–10415.

(16) (a) Kuiper, J. M.; Engberts, J. B. F. N. *Langmuir* **2004**, *20*, 1152–1160. (b) Deng, Y.; Li, Y.; Wang, X. *Macromolecules* **2006**, *39*, 6590–6598.

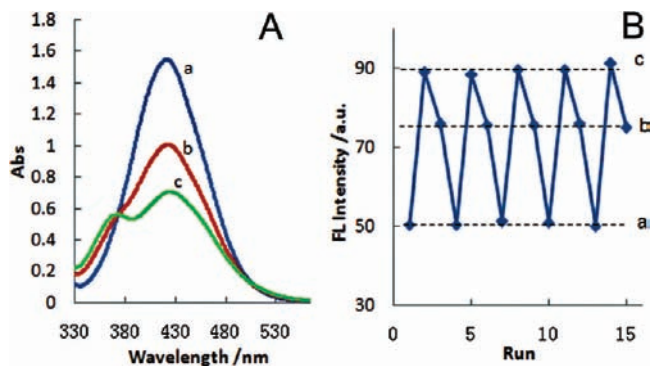


Figure 3. Photoresponsivity of TA and TA-capped CdS QDs in THF. (A) UV-vis absorption spectra of the TA ligand: (a) relaxed in a dark chamber overnight; (b) under UV exposure; (c) under visible-light exposure. (B) Dependence of the intensity of fluorescence band Q on the photoisomerization conditions. The labels have the same meanings as in (A).

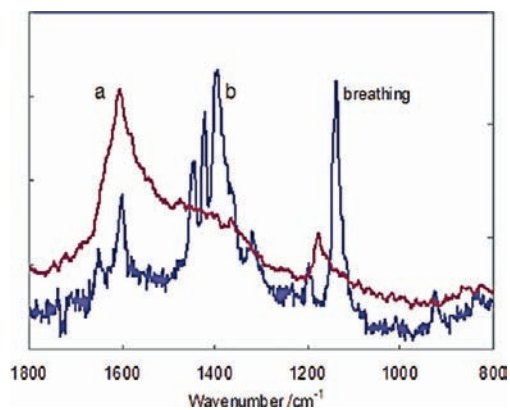


Figure 4. Raman spectra of TA-capped CdS QDs excited at (a) 325 and (b) 514.5 nm.

C is not related to the azobenzene group in the TA ligand and thus is related to the complexes of the 1,2,3-triazole groups in TA.

Complexation of TA with CdS. Spectroscopy is a powerful technique for characterizing charge-transfer (CT) bands. The observed X-ray photoelectron spectroscopy (XPS) and Raman spectroscopy properties of TA-capped CdS QDs support the formation of CT complexes between the 1,2,3-triazole groups of TA and the surface Cd atoms of CdS QDs. Raman analysis of the QDs at different excitation wavelengths (325 and 514.5 nm) was performed (Figure 4). Usually, longer excitation wavelengths are more suitable for obtaining information deeper inside the surface, and the Raman spectrum of QDs excited at 514.5 nm was nearly the same as that of pure TA. The strong peak at 1139 cm⁻¹ excited at 514.5 nm was assigned to the breathing mode of the 1,2,3-triazole rings,¹⁷ which showed a significant blue shift to 1179 cm⁻¹ upon excitation at 325 nm. The blue shift for triazole groups attached on the QD surface can be attributed to strengthening of the triazole rings as they obtain electrons upon formation of the CT complexes, in which the triazole rings are the electron acceptors.

The XPS results (Figure 5) clearly showed that the N 1s peak of the TA ligand moved to lower energy upon binding to the surface of QDs, shifting from 400 eV (pure TA) to 399.5 eV (TA-conjugated CdS QDs); this means that nitrogen atoms

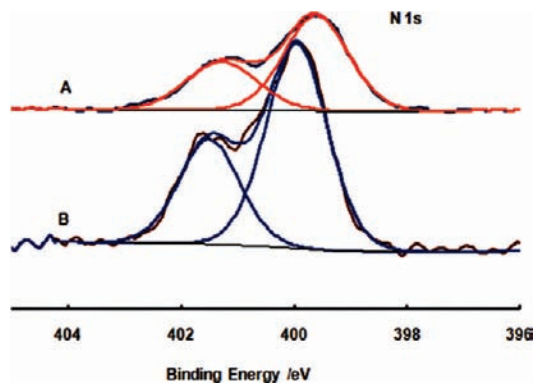


Figure 5. XPS N 1s peaks in (A) TA-conjugated CdS QDs and (B) pure TA.

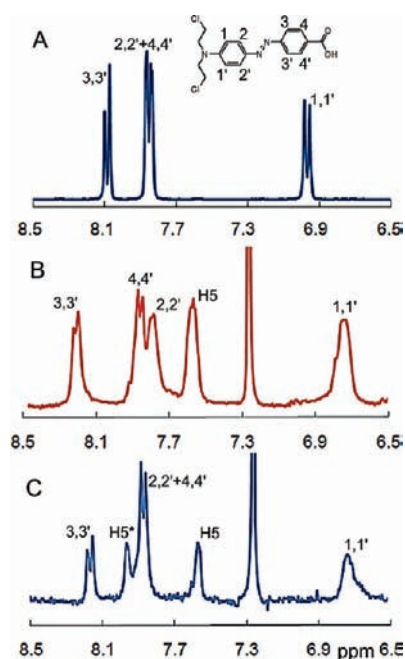


Figure 6. ¹H NMR aromatic signals of (A) the TA precursor BAA (in DMSO-*d*₆), (B) TA, and (C) TA-capped CdS (in CDCl₃). Peak H5 arises from the proton on 1,2,3-triazole cycle and peak H5* from the proton of 1,2,3-triazole group conjugated with CdS.

accepted electrons in the formation of the CT complexes. The XPS results revealed that 1,2,3-triazole groups do not interact with CdS as Lewis bases by dative bonding. Donation of electrons or bearing positive charges would cause the binding energies of the nitrogen atoms to shift to higher energy.

Deeper insight into the molecular interactions was gained via analysis of the aromatic portion of the ¹H NMR spectra of TA and TA bound to the surface of CdS QDs (Figure 6). To help in the assignment of the NMR peaks, the ¹H NMR spectrum of the small precursor molecule 4-[[bis(2-chloroethyl)amino]phenylazo]benzoic acid (BAA) is also presented (Figure 6A). In the NMR spectrum of BAA, the coupling constants ³J₃₄ (between the adjacent protons 3 and 4) and ³J₁₂ (between the adjacent protons 1 and 2) were ~9 Hz. The chemical shifts of protons 2, 2', 4, and 4' were nearly the same. The ratios of peak integrals were 2,2'+4,4'/3,3'/1,1' = 4:2:2. In the NMR spectrum of TA, the proton on the 1,2,3-triazole cycle gave rise to the peak at 7.55 ppm (peak H5 in Figure 6B). ³J₃₄ was not changed. However, ³J₁₂ obviously decreased, leading to degenerate peaks for 1 and 1' and for 2 and 2'. Protons

(17) Jbarah, A. A.; Ihle, A.; Banert, K.; Holze, R. *J. Raman Spectrosc.* **2006**, *37*, 123–131.

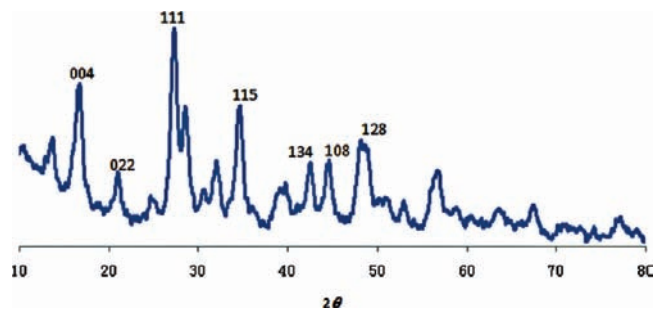


Figure 7. Powder XRD pattern for the 1,2,3-triazole–Cd(II) complex.

2 and 2' were shifted to higher field and isolated from 4 and 4' by ~ 0.06 ppm. The ratios of peak integrals remained $2,2'/4,4'/3,3'/1,1' = 4:2:2$, and the integral of peak H5 corresponded to two protons due to the bidentate click cycles.

As a result of complexation of TA with CdS, the aromatic protons were shifted a little bit upfield (Figure 6C). Protons 2 and 2' overlapped with 4 and 4' again, as evidenced by the $2,2'+4,4'/3,3'/1,1'$ ratios of peak integrals. $^3J_{34}$ was affected hardly at all by surface conjugation. The most significant change in the spectrum of TA bound to CdS was the newly appearing singlet peak at 8.0 ppm, which was assigned to the proton of the 1,2,3-triazole groups conjugated with CdS (H5* in Figure 6C). The sum of the integrals for H5 and H5* was equal to that for 3,3' or 1,1'. The downfield shift ($\Delta\delta$) of H5* relative to H5 was ~ 0.45 ppm. Kogot et al.¹⁸ observed a downfield shift of ~ 0.2 ppm for HIS protons due to complexation of HIS with a gold surface. The downfield shift of ligand protons is a direct evidence of molecular coordination. The H5/H5* integral ratio was $\sim 0.55:0.45$, which meant that $\sim 45\%$ of 1,2,3-triazole groups were involved in surface conjugation. TA conjugation formed a monolayer of TA over the CdS surface. Additional TAs were adsorbed around the CdS QDs or dissolved in the aqueous solutions.

To further investigate the complexation of 1,2,3-triazole groups of TA with the surface Cd atoms of CdS, we used the small molecule 1,2,3-triazole as the model compound. 1,2,3-Triazole formed an insoluble complex with Cd(II) in ethanol, whereas both 1,2,3-triazole and cadmium(II) acetate are soluble in ethanol. The crystal structure of the 1,2,3-triazole–Cd(II) complex was explored using powder XRD (Figure 7). The powder XRD patterns were indexed according to the following procedure: first, a best-fit crystalline structure was found using the Monte Carlo simulation software McMaille,¹⁹ and then the patterns were indexed according to the best-fit parameters using a powder indexing helper tool, chekcell.²⁰ The best fit was an ortho structure ($a = 2.78$ Å, $b = 7.18$ Å, $c = 15.55$ Å).

The complexation between 1,2,3-triazole and Cd(II) ions was further studied by cyclic voltammetry (CV) and conductometric titration experiments. The titration conductance method for measuring the formation constants of the complexes between alkali-metal ions and crown ethers has been established.²¹ According to the same method, we measured the formation

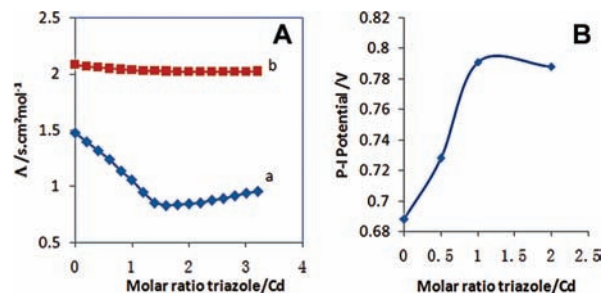


Figure 8. Electrochemical analysis of the complexation of 1,2,3-triazole and Cd(II) ions. (A) (a) Conductance change upon titration of 1,2,3-triazole into cadmium acetate/ethanol solutions; (b) theoretical summation of the conductivities of 1,2,3-triazole and cadmium acetate at the same concentrations as in (a). (B) Change in CV oxidation peak potential of 1.25 mM CdCl₂ in aqueous 0.1 M KNO₃ upon addition of 1,2,3-triazole.

constant of the complex of 1,2,3-triazole and Cd(II) ions. The molar conductivity (Λ) is plotted versus [1,2,3-triazole]/[Cd(II)] molar ratio in Figure 8A. According to the titration-conductance experiments, a complex with structure of $[(1,2,3\text{-triazole})_{1.5}\text{Cd(II)}]_x$ was formed, and the formation constant was calculated as $\log(K_f) = 3.97$.

CV experiments on aqueous solutions of CdCl₂ in the absence or presence of 1,2,3-triazole were performed. The CV method for studying metal ion complexes has also been established.²² Figure S2 in the Supporting Information shows the cyclic voltammograms of CdCl₂ versus a Ag/AgCl reference electrode. A peak potential (P-I) of ~ 0.69 V due to oxidation of the Cd atoms was observed. When 1,2,3-triazole was added, the P-I peak became more positive and reached a maximum (0.79 V) at 1,2,3-triazole/Cd(II) = 1 (Figure 8B), which meant that it was more difficult for Cd metal to donate electrons but easier for Cd(II) to accept electrons. According to the above Raman and XPS results, the triazole rings act as electron acceptors in forming the metal-to-ligand CT (MLCT) complex.²³ Thus, because of complexation with 1,2,3-triazole, the Cd atoms that have donated electrons to 1,2,3-triazole are more difficult to oxidize (losing electrons); however, Cd(II) ions more easily accept electrons on the contrary. The MLCT was also observed in 1,2,3-triazole ligands through click reactions and their palladium and platinum complexes.²⁴

Stability of TA-Capped QDs. Aqueous solutions of TA-capped CdS QDs were stable during storage for 1 year. To further investigate the stability of TA-capped QDs, the photofluorescence properties of TA-capped QDs at different ionic strengths were monitored as the concentration of KCl was increased from 0 to 1.0 M while the QD concentration was kept constant. The solutions were stored at room temperature for 1 day before photofluorescence analysis. Over the concentration range of KCl used (0–1.0 M), we observed no change in either the photoluminescence intensities or the characteristics of the emission spectra (Figure 9A).

In addition, we investigated the pH stability of aqueous dispersions of TA-capped CdS QDs. CdS dispersions in Tris-HCl/NaOH buffers at various pH (1.0, 3.0, 5.0, 7.0, 9.0, 11.0, and 13.0) were stored at room temperature for 1 day before photofluorescence analysis. Figure 9B,C demonstrates the effects

(18) Kogot, J. M.; England, H. J.; Strouse, G. F.; Logan, T. M. *J. Am. Chem. Soc.* **2008**, *130*, 16156–16157.

(19) Le Bail, A. *Powder Diffraction*. **2004**, *19*, 249–254.

(20) Laugier, J.; Bochu, B. *LMGP Suite: A Suite of Programs for the Interpretation of X-ray Experiments*; ENSP/Laboratoire des Matériaux et du Génie Physique: Saint Martin d'Hères, France, 2004; <http://www.ccp14.ac.uk/tutorial/lmgp/>.

(21) Takeda, Y.; Yano, H.; Ishibashi, M.; Isozumi, H. *Bull. Chem. Soc. Jpn.* **1980**, *53*, 72–76.

(22) Hume, D. N.; Deford, D. D.; Cave, G. C. B. *J. Am. Chem. Soc.* **1951**, *73*, 5323–5325.

(23) Castellano, F. N.; Malak, H.; Gryczynski, I.; Lakowicz, J. R. *Inorg. Chem.* **1997**, *36*, 5548–5551.

(24) Schweinfurth, D.; Pattacini, R.; Strobel, S.; Sarkar, B. *Dalton Trans.* **2009**, 9291–9297.

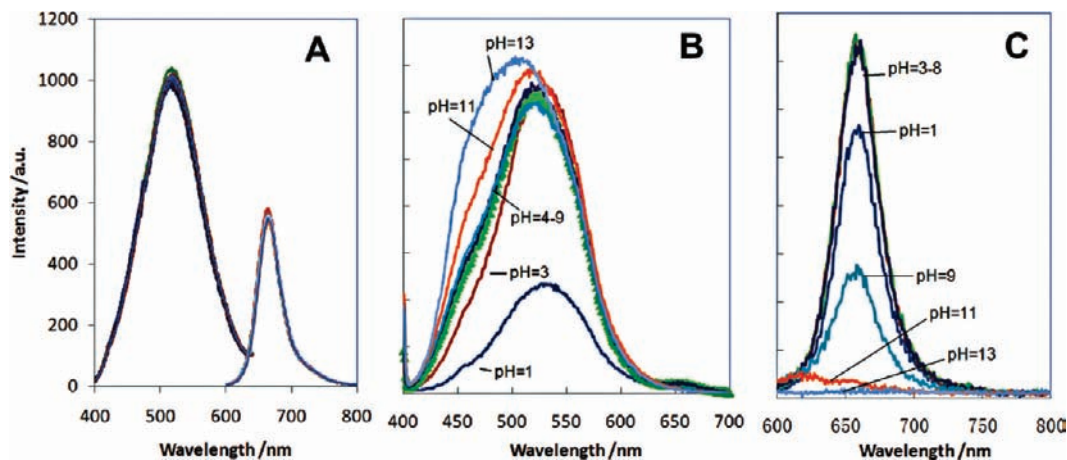


Figure 9. Effect of increasing (A) the ionic strength and (B, C) the pH (in Tris buffers) on the photoluminescence of TA-capped CdS QDs. In (A), the dispersions of QDs contained equal concentrations of QDs but various concentrations of KCl (0.0, 0.2, 0.4, 0.6, 0.8, and 1.0 M). (B) shows results for band Q, and (C) gives results for band C.

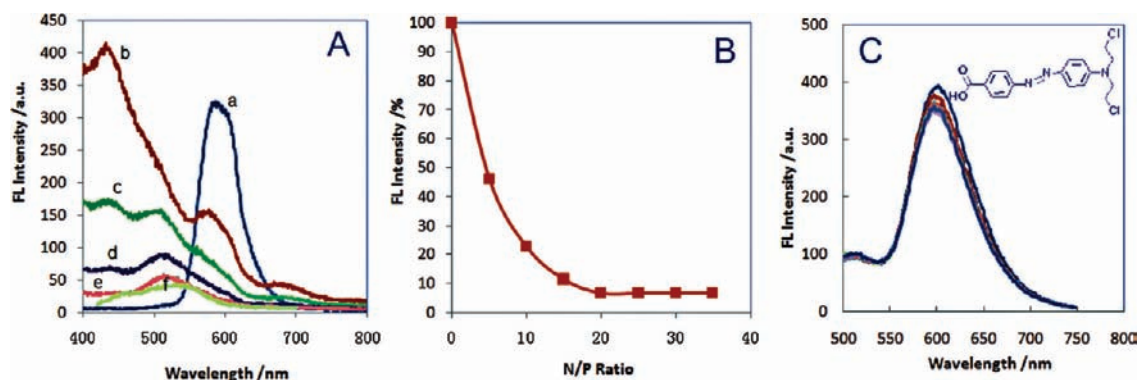


Figure 10. Ethidium bromide exclusion assay for TA-ct-DNA complexes. The solutions were mixed at various [1,2,3-triazole groups of TA]/[DNA phosphate] (N/P) ratios. (A) (a) free DNA + ethidium bromide; (b–e) N/P = 5, 10, 15, and 20, respectively; (f) TA ligand. (B) Change in DNA–EB complex fluorescence upon addition of TA. (C) EB–ct-DNA exclusion assay for TA precursor BAA.

of increasing pH values on fluorescence bands Q (arising from CdS) and C (arising from the surface complexes) of TA-capped CdS QDs. Over a broad range of pH (pH 3–8), we observed little or no change in either the fluorescence intensities or the characteristics of the emission spectra for either band Q or band C. Over the pH range 3–13, the fluorescence intensity of band Q did not decrease, though a small blue shift happened. This indicated that the ligand TA was a good protective agent for the CdS nanocrystals. Band C seemed more sensitive to basic pH. At pH above 11, band C disappeared. The difference in pH stability of bands Q and C is related to the different chemical natures of the fluorophores from which the bands are emitted. CdS is a very stable inorganic dye, but it is apt to dissociate under strongly acidic conditions. Thus, band Q is stable over a broad range of pH except around pH 1. Band C is emitted from surface complexes that can dissociate in a rigorous pH range.

Overall, the aqueous dispersions of TA-capped CdS QDs were stable in physiological environments. In the other hand, the different pH sensitivities of bands Q and C in the same QDs might supply the ability to control a certain color during multicolor imaging. This is also a desirable property when using inorganic nanoparticles as delivery vectors for genes, drugs, or analytical reagents.²⁵

Interaction of the TA Ligand with ct-DNA. The TA ligand can strongly interact with DNA, as demonstrated by an ethidium bromide (EB) exclusion assay using calf thymus DNA (ct-DNA) as the model DNA (Figure 10). Free EB emits very weak

fluorescence; however, EB is positively charged and can bind free DNA plasmids to form complexes having strong fluorescence at ~600 nm. EB cannot bind plasmids that are already strongly complexed with other compounds.²⁶ According to Figure 10, at a 1,2,3-triazole group to phosphate (N/P) ratio of 5, the fluorescence of the DNA–EB complex was decreased by 50%, indicating a strong interaction between DNA and the TA ligand. DNA was retarded at an N/P ratio of 15–20 (Figure 10B). A newly appearing strong fluorescence peak at 438 nm arising from the TA–DNA complex also supported the strong interaction between TA and DNA (Figure 10A).

To further experimentally confirm that the strong interaction with DNA arose from the click cycles and not from the azobenzene groups, we carried out a side-by-side comparison experiment using the precursor BAA in the EB exclusion assay. Condensation of ct-DNA by the precursor did not take place, nor did the fluorescence peak at ~440 nm appear. Thus, we concluded that the strong interaction with DNA arose from the 1,2,3-triazole groups.

Staining of Cancer Cells. We used TA-capped CdS QDs to stain fixed cancer cells. Three kinds of cancer cells were tested: human cervical carcinoma (HeLa), human lung carcinoma

(25) (a) Radu, D. R.; Lai, C. Y.; Jeftinija, K.; Lin, V. S.-Y. *J. Am. Chem. Soc.* **2004**, *126*, 13216–13217. (b) Luo, D.; Saltzman, W. M. *Nat. Biotechnol.* **2000**, *18*, 893–895. (c) Shen, H.; Tan, J.; Saltzman, W. M. *Nat. Mater.* **2004**, *3*, 569–574.

(26) Tang, M. X.; Szoka, F. C. *Gene Ther.* **1997**, *4*, 823–832.

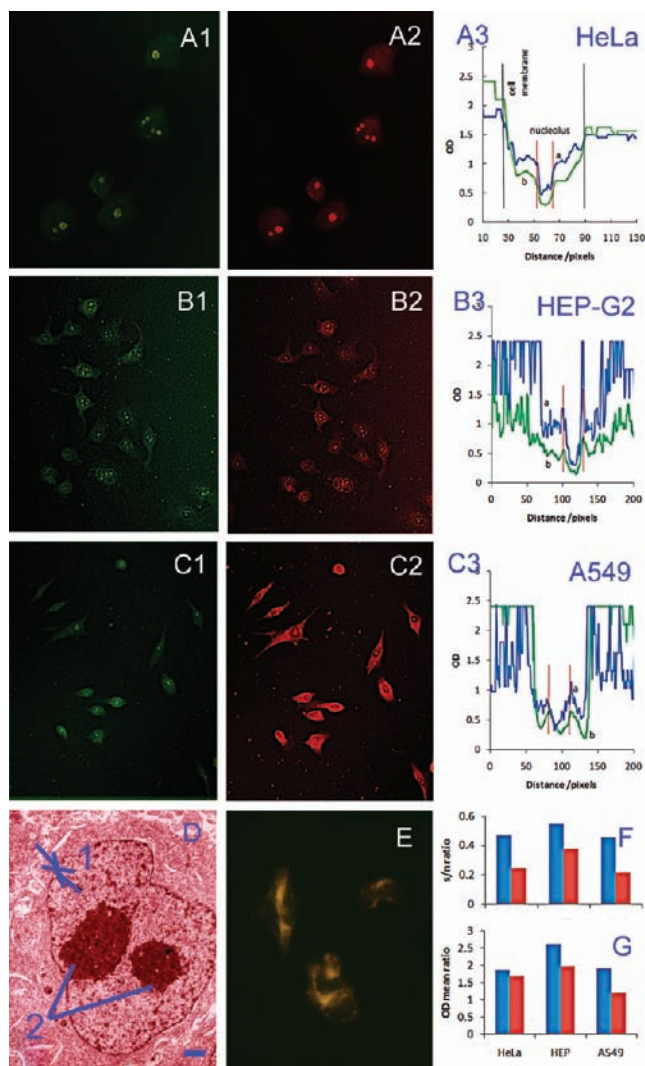


Figure 11. Fluorescent micrographs and a TEM image of QD-stained cancer cells. Except for the control test (E), all of the results were obtained for cancer cells stained with TA-capped CdS QDs. (A1–2) HeLa; (B1–2) HEP G2; (C1–2) A549. A1–C1 were excited with blue light and (A2–C2) with green light. (D) TEM image of a HeLa cell stained with TA-capped QDs: (1) nuclear membrane; (2) QD-stained nucleoli. The scale bar represents 1 μm . (E) Control test in which HeLa cells were stained with thioglycolic acid-capped CdS QDs. (A3–C3) Line profiles of single cells in fluorescent micrographs excited by (a) blue and (b) green light. (F) Signal-to-noise ratio (nucleolus signal to cytoplasm signal). (G) Ratio of area-averaged fluorescence intensities (nucleolus to the whole cell).

(A549), and human liver carcinoma (HEP G2). Figure 11 displays fluorescent micrographs of cancer cells stained using the TA-conjugated CdS QDs. These QDs emitted an olive color under excitation with blue light (Figure 11A1–C1) but emitted in situ red light under excitation with green light (Figure 11A2–C2). The in situ dual-color fluorescence further proved that the red fluorescence arose from the surface complexes and that the surface complexes were strong enough in the cellular environment.

Notably, fluorescent micrographs showed that the TA-conjugated QDs had a strong affinity for cancer cell nucleoli. The fluorescence dots were highly concentrated in the nucleoli of the three kinds of cancer cells. To further investigate the location of the QDs, we made ultrathin epoxy resin sections of HeLa cells stained by TA-capped QDs for TEM observation. The TEM image clearly showed that TA-capped QDs were

preferentially concentrated in the cell nucleoli. As a control experiment, thioglycolic acid-capped CdS QDs were produced and used for staining HeLa cells according to the same procedure. The fluorescent micrograph (Figure 11E) showed that the thiol-ligand-conjugated QDs stained mainly the cell membranes and could not pass the cell membranes to reach the cell nucleoli.

To evaluate the signal-to-noise (s/n) ratio for the staining by TA-capped QDs, line profiles of single cells along a horizontal line crossing a nucleolus were plotted (Figure 11A3–C3) and clearly showed the optical densities of background (OD_b), cytoplasm (OD_c), and nucleolus (OD_n). We calculated the s/n ratio for the nucleolus signal relative to the cytoplasm signal using eq 1:

$$\text{s/n ratio} = \frac{OD_c - OD_n}{OD_b - OD_c} \quad (1)$$

The average results for each kind of cell are plotted in Figure 11F. Staining by TA-conjugated QDs had acceptable s/n ratios for the three kinds of cancer cells, and in particular, blue-light excitation (s/n ratio > 0.4) was better than green-light excitation. This was because the red fluorescence from band Q had higher quantum yields, and thus, the fluorescence from the background and cytoplasm was increased.

We also characterized the specificity of QDs bound to the nucleoli by comparing the area-averaged fluorescence intensity of the nucleoli relative to a whole single cell according to the OD mean ratio, which is the ratio of the area-averaged fluorescence intensity from the nucleolus to that from the whole cell including the nucleolus. The area-averaged fluorescence intensity was obtained from the mean OD in a negative fluorescence picture. The OD mean ratios are plotted in Figure 11G for the three kinds of cells. The values varied around 1.9 for both band Q and band C (i.e., the mean fluorescence intensity from a QD-stained nucleolus was ~ 1.9 -fold that from a whole cell). TA-capped QDs showed a strong preference for binding to the nucleolus.

Because of the importance of visualizing cell nucleoli, many selective staining techniques for nucleolar materials have been developed. Generally, these techniques can be categorized into two groups: those that target nucleolus-specific proteins, including NoLS polypeptides and antibodies to specific proteins,²⁷ and those that target the genetic materials (DNA or RNA).²⁸ Yu et al.²⁹ found that a europium complex selectively stained nucleoli of cells, and a strong interaction of the europium complex with serum albumin was supposed to be the driving force for selective location of the dye. However, it is a complicated case for nucleolar-targeting QDs. Both suitable size for cell permeability and specific interaction with nucleolar materials are important for QDs to achieve the nucleolar-targeting function. Because of the strong interaction of TA with DNA, it is reasonable to suppose that a strong interaction of TA with nucleic acids was the driving force of the nucleolar-

(27) (a) Dean, K. A.; von Ahnen, O.; Görlich, D.; Fried, H. M. *J. Cell Sci.* **2001**, *114*, 3479–3485. (b) Korgaonkar, C.; Hagen, J.; Tompkins, V.; Frazier, A. A.; Allamargot, C.; Quelle, F. W.; Quelle, D. E. *Mol. Cell Biol.* **2005**, *25*, 1258–1271.

(28) (a) Liu, X.; Chen, H.; Patel, D. J. *J. Biomol. NMR* **1991**, *1*, 323–347. (b) Li, Q.; Kim, Y.; Namm, J.; Kulkarni, A.; Rosania, G. R.; Ahn, Y.-H.; Chang, Y.-T. *Chem. Biol.* **2006**, *13*, 615–623.

(29) Yu, J.; Parker, D.; Pal, R.; Poole, R. A.; Cann, M. J. *J. Am. Chem. Soc.* **2006**, *128*, 2294–2299.

targeting functions of TA-capped QDs. A detailed study of the nucleolar-targeting functions of TA will be carried out in the future.

Conclusions

The bidentate 1,2,3-triazole-based ligand TA synthesized in this work is a multifunctional ligand for stabilizing CdS QDs in aqueous environments with different ionic strengths over a broad pH range, including cellular environments. Because of the formation of fluorescent surface complexes, TA-capped CdS QDs could change fluorescence in situ, emitting olive light (arising from CdS nanocrystals) when excited with UV or blue light and emitting red light (arising from the surface complexes) when excited with green light. Fluorescence micrography and TEM analysis showed that TA-capped CdS QDs had nucleolar-targeting properties. It is supposed that a strong interaction

between TA and nucleic acids was the driving force of the nucleolar-targeting functions of TA. The nucleolus is a critical regulator of many cellular functions and is also emerging as an important target of various viral proteins (e.g., the HIV virus). Thus, our work would be interesting for research in a broad range including bioassays, gene therapy, antiviral drugs, and so on.

Acknowledgment. Support from the National Natural Science Foundation of China (Project 50773076) is acknowledged.

Supporting Information Available: Experimental section and Figures S1 and S2. This material is available free of charge via the Internet at <http://pubs.acs.org>.

JA1002668